SECTION V

Functional Extracts and Force Measurements

CHAPTER 29

Quantitative Characterization of Filament Dynamics by Single-Molecule Lifetime Measurements

Leonid A. Mirny* ***and*** **Daniel J. Needleman†**

*Harvard-MIT Division of Health Sciences and Technology, and Department of Physics, Massachusetts Institute of Technology, Cambridge, Massachusetts 02139

†Molecular and Cellular Biology, School of Engineering and Applied Sciences, FAS Center for Systems Biology, Harvard University, Cambridge, Massachusetts 02138

Abstract

Single-molecule measurements provide a powerful tool for obtaining quantitative information on biological process. However, properly interpreting these measurements can be challenging. Here we present a framework for understanding the turnover dynamics of single molecules in cytoskeletal filaments. We show that the single-molecule lifetime distribution is equivalent to the distribution of first-passage times of the filaments ends. We calculate expected lifetime distributions for a number of models of filament dynamics. We also describe methods to measure single-molecule turnover of tubulin molecules in Xenopus egg extract spindles. We show

METHODS IN CELL BIOLOGY, VOL. 95

978-0-12-374815-7
DOI: 10.1016/S0091-679X(10)95029-2

that analyzing the shape of the lifetime distribution gives insight into the mechanism of microtubule turnover in these spindles and can be used to quantify the effect of molecular perturbations on microtubule stability. Similar methods should prove useful in studying cytoskeletal filaments in other contexts *in vitro* and *in vivo*.

I. Introduction to Cytoskeletal Filament Dynamics

The cytoskeleton is used by cells in an astonishing variety of contexts, including cellular organization, motility, and division (Alberts *et al*., 2008). Many of these behaviors depend on the polymerization and depolymerization of cytoskeletal filaments. Both actin and microtubules primarily lose and gain subunits from their ends, and both these filaments can sever, generating new ends, or anneal. Despite tremendous effort, the biophysical basis of cytoskeletal filament turnover is still not well understood. Discrete state, chemical kinetic models are often used to describe the behavior of these polymers, but there is increasing evidence that their true dynamics are quite complicated and may involve intricate structural and mechanical transitions which cannot be easily represented by such simple theories (Kueh and Mitchison, 2009). Our current deficiencies in understanding these systems are partly due to their shear complexity and partly due to our lack of experimental and theoretical tools capable of measuring and interpreting the relevant dynamics.

Even more mysterious than individual cytoskeletal filaments is the process by which the interactions between these polymers give rise to cellular-scale behaviors. Many regulatory proteins interact with cytoskeletal filaments in cells, greatly modulating their activities, so the dynamics of actin and microtubules in complex, cellular systems may be quite different from what they are in solutions of purified components. Thus it is crucial to obtain measurements of filament dynamics inside the structure of interests. For example, despite being studied for over 60 years, we still do not understand how microtubules behave in spindles; we do not know how microtubule nucleation is regulated, the importance of microtubule severing and annealing, the extent to which microtubule lengths and stability are spatially controlled, and the relative contribution to turnover of the plus and minus ends (Dumont and Mitchison, 2009). Many of these questions could be answered if it were possible to directly observe the behaviors of individual microtubules in spindles, but unfortunately, their density is so high that they cannot be optically resolved. A variety of techniques—including the response of the spindle to perturbations (Inoue and Sato, 1967), fluorescent recover after photobleaching (FRAP) (Salmon *et al*., 1984), and photoactivation (Sawin and Mitchison, 1991)—have revealed that microtubules' turnover is very rapid in spindles, but the mechanism of turnover has not been fully established. While speckle microscopy, in which only a small fraction of molecules are labeled, has recently been used to great effect to study microtubules in spindles (Valloton *et al*., 2003), it is still not entirely clear how to relate these measurements to the behavior of individual microtubules. Single-molecule measurements are simpler than speckle microscopy to analyze because each molecule will only be incorporated in a single microtubule. Still, there is only an indirect relationship between the behavior of single molecules, which can be observed, and the underlying dynamics of microtubules, which are of interest, so some theory must be used to interpret these measurements. In this article, we describe single-molecule

tracking experiments of tubulin molecules *in vitro* spindles, and we present a theoretical framework that allows this data to be meaningfully interpreted. We believe that these methods should be useful for studying other systems as well and provide a basis for analyzing single-molecule measurements in polymer systems more generally.

II. Single-Molecule Lifetime Measurements

A. Extract and Sample Preparation

Xenopus egg extracts were prepared following standard protocols (Hannak and Heald, 2006). All of our data was acquired on spindles assembled from sperm nuclei after one round of DNA replication, but similar experiments can be performed with spindles assembled without DNA replication or with other sources of DNA, such as bead spindles (unpublished). Tubulin was purified from cow brains and directly labeled with alexa-647 using the procedure of Hyman *et al*. (1991). The alexa-647 tubulin was added to extracts to a final concentration of ~0.15 nM. Adding tubulin before or after spindle assembly produced similar results. Hoechst was added to label DNA, which allowed easy identification of spindles.

Samples for microscopy were prepared by placing 4–6 μl of spindle reaction on a slide, covering the solution with an 18 × 18-mm coverslip (#1.5), and sealing with candle wax or valap. Sealing is important to prevent flows in the sample that can cause motion of the spindle, making analysis difficult. Furthermore, there is substantially less photobleaching in sealed samples, presumably because of active sequestering of oxygen by the extract (Niethammer *et al*., 2008).

B. Microscopy

We imaged with a spinning disk confocal microscope (CSU-10, Yowkogawa) mounted on an inverted microscope (E800, Nikon), with 60× or 100× oil immersion objectives (1.4 numerical aperture, plan apo, differential interference contrast; Nikon). Excitation was provided by the 647 line of an argon–krypton mixed gas laser with a total power of ~3 mW after the objective. Movies were recorded with back-illuminated electron multiplying CCDs (iXonEM+ 897 or iXonEM 860, Andor) operated with maximum EM gain. These cameras have excellent quantum efficiency (above 90% for wavelength between ~500 and 700 nm), very low dark current due to intense cooling (which we set to –80°C), and negligible effective read noise because the signal is amplified (nearly 1000-fold) before it is read by the analog-to-digital converter. However, the gain process is stochastic, leading to a multiplicative noise that makes the camera function as a detector with no noise but half the quantum efficiency. We therefore acquired images by averaging together 16 separate 100-ms exposures (with streaming acquisition, i.e., no shuttering), a procedure that would be counterproductive if read noise was significant.

Modern microscopes and detectors are of such high quality that the major challenges in single-molecule imaging are more often associated with sample preparation than with optics. Xenopus egg extracts, like many biological samples, are autofluorescent, which generates a large background in the green. The extracts' autofluorescence decreases with increasing wavelength, so using red-shifted dyes greatly

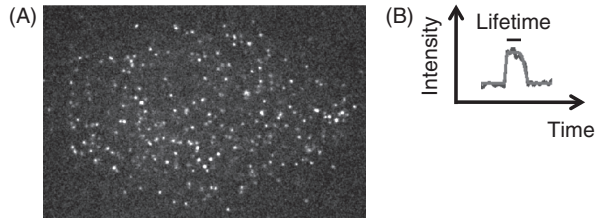

Fig. 1 Single-molecule imaging in spindles. (A) An image of a spindle with single molecules of tubulin visible. (B) The fluorescence intensity of a single molecule (blue curve) shows a step-like change (red line). A molecules lifetime is the amount of time it spends in the spindle.

improves imaging quality. Because of this issue, we have found that rhodamine is substantially better than alexa-488 for single-molecule imaging in Xenopus egg extract, and alexa-647 is better still.

For single-molecule imaging, it is not only necessary to select the correct fluorophore, but also essential to use the right concentration of labeled molecules. If the concentration is too high, then single molecules cannot be resolved and the fluorescence from cytoskeletal-bound molecules of interest might be swamped by the signal from soluble fluorophores. If the concentration of fluorophores is too low, then it may take prohibitively long to interrogate a sufficient number of molecules to collect good statistics. An estimate to keep in mind is that a 1 nM solution will have approximately one molecule per diffraction limited volume. We have found that using a labeled tubulin concentration of ~0.1 nM is a good comprise.

Images of spindles with ~0.1-nM-labeled tubulin show well-defined, discrete points of fluorescence with Gaussian intensity profiles (Fig. 1A). Qualitatively similar pictures can result for sparse labeling even if the particles are not actually single molecules, so care must be taken in interpreting these images. There are a number of ways to demonstrate that the observed particles really are single molecules: (1) For low concentration, the intensity of particles does not depend on their density; (2) particles appear and disappear in a step-like fashion; and (3) when photobleaching is induced, particles disappear with single exponential kinetics (though bleaching is negligible under our standard imaging conditions). All of these criteria are met for ~0.1-nM-labeled tubulin in Xenopus egg extract spindles (Needleman *et al*., 2010; Yang *et al*., 2007).

C. Data Analysis

Movies of tubulin molecules in spindles reveal that the molecules undergo constant motion and appear and disappear. These behaviors are best studied using automated particle tracking techniques to collect extensive statistics. Automated particle tracking typically consists of two components: first, particles are identified in each frame of a movie; second, these particle locations are linked over time to form trajectories. Sophisticated methods can be used to identify and track particles even when they partially overlap (Jaqaman *et al*., 2008; Serge *et al*., 2008). However, such methods use models of particle dynamics which might be incorrect and therefore could introduce subtle errors in the resulting particle trajectory. While it is

possible to optimize the tracking algorithms to minimize such mistakes, we have taken the more conservative approach of working at very low particle density and disregarding particles which cross each other. This enables us to use relatively simple tracking algorithms at the cost of reduced statistics (Crocker and Grier, 1996).

We will not discuss the analysis of particle motions in this article; our focus is on understanding appearance and disappearance. We have previously demonstrated that apparent appearance and disappearance of tubulin molecules is caused by tubulin turnover in the spindle and is not due to movement of molecules in and out of focus or photobleaching. Particle appearance is caused by a soluble fluorescent tubulin molecule being incorporated into a microtubule while particle disappearance occurs when the fluorescent tubulin molecule dissociates from a microtubule. We refer to the total amount of time that a particle is in a microtubule, the time between appearance and disappearance, as its lifetime (Fig. 1B). Measuring the distribution of lifetimes provides detailed information on the mechanism and timescales associated with tubulin turnover. Before presenting our experimental results, we will describe a theoretical framework that allows the measured lifetime distribution to be related to models of microtubule behavior.

III. Theoretical Foundations

A. Equivalence to the First-Passage Time Problem

Our approach to quantitative analysis of single-molecule experiments is based on an idea that establishes a rigorous parallel between single molecule appearing/disappearing at the tip of the growing filament and the first-passage time (FPT) of the corresponding stochastic process. This connection is shown in Fig. 2. Consider a tip of a single filament that grows and shrinks stochastically. The association of a labeled monomer molecule to the growing tip leads to the appearance of a new speckle. The speckle will stay attached and, hence, visible until the monomer is lost during one of the rounds of depolymerization. If we describe the dynamics of the growing filament as a stochastic process (e.g., a random walk of some sort), then the

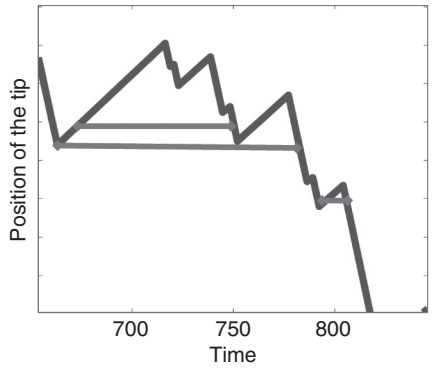

Fig. 2 Equivalence of speckle lifetime and first-passage (return) time. Trajectory of the dynamic tip of a filament is shown in gray, with the speckle lifetimes shown by red intervals.

lifetime of a single particle equals the time interval between the moment that the trajectory passes a certain coordinate while growing (association) and the moment when it returns to the same coordinate for the first time while shrinking (dissociation), i.e., *the FPT*. Note that many rounds of growth and shrinkage can take place before the filament loses a specific labeled monomer.

The equivalence between the molecular lifetime and the FPT of the stochastic trajectory that characterizes filament dynamics allows one to make several quantitative measurements. First, given a model of filament dynamics (see later) one can calculate the distribution of FPT for that process. FPT distributions computed for different models of the process can then be compared with experimentally obtained single-molecule lifetime (SLT) distribution, providing a test of the validity of different models of filament dynamics. Second, parameters that characterize filament dynamics (e.g., growth and switching rates) can be determined by fitting the measured SLT distribution to the predicted form of the FPT distribution. Third, by comparing SLT distributions obtained at different locations of the cell one can quantitatively compare filament dynamics at these locations. Fourth, experiment that affects growth rates and other dynamic parameters can be used to further interrogate filament dynamics by comparing predicted and observed changes in FPT and SLT distributions. These and other methods are discussed later.

B. Models of Filament Dynamics

Models of filament dynamics aim at describing stochastic dynamics of the filament growth and shrinkage. If predominantly one end is subject to polymerization and depolymerization, then dynamics is given by $p(x, t)$, the probability of having this end at coordinate x at time t. Given $p(x, t)$ one can calculate the desired FPT distribution (Redner, 2001) and compare it to the experimental SLT distribution. We examine a number of models of filament dynamics below.

1. Diffusion with Drift

We start by considering a model where only one of the filament ends is subject to polymerization and depolymerization. In general, dynamics of the tip can be considered as a one-dimensional (1D) random walk. If individual events of polymerization and depolymerization are uncorrelated (or are considered at times longer than the correlation times) the evolution of the probability $p(x, t)$ can described by the Fokker–Planck equation:

$$\frac{\partial p(x,t)}{\partial t} = -V\frac{\partial p(x,t)}{\partial x} + D\frac{\partial^2 p(x,t)}{\partial x^2} \tag{1}$$

where V is the drift velocity, which characterizes the tendency of the filament to grow ($V > 0$) or shrink ($V < 0$), and D is the diffusion coefficient, which quantifies the magnitude of fluctuations. If $V > 0$ the filaments grow continuously and have no steady-state distribution. If $V < 0$ the filaments shrink and a steady state can be maintained where nucleation balances depolymerization. In this case, the lengths of the filaments will be exponentially distributed with mean $L = D/V$.

The diffusion-with-drift process can be considered as a 1D random walk performed by the tip of the filament and characterized by two parameters: the diffusion coefficient of the random walk and the velocity of the drift. Note that individual steps of the random walk do not necessarily correspond to individual events of monomer association and dissociation. For example, in the case of microtubule dynamic instability, alternating periods of growth and shrinkage might act as "steps" of the random walk.

At timescales longer than times of individual steps, the FPT distribution (more precisely, the *return time* distribution) for a random walk with nonzero drift ($V \neq 0$) is

$$f(t) = At^{-3/2} \exp(-t/\tau), \quad \tau = \frac{4D}{V^2} \tag{2}$$

where A is a time-independent constant. At short timescales the distribution behaves as a power law $f(t) \sim t^{-3/2}$, while at longer timescales it starts decaying exponentially $\sim \exp(-t/\tau)$ with a single timescale τ. This timescale determines the balance between velocity and drift (i.e., between deterministic and stochastic effects). In the absence of drift, the distribution converges to that of the unbiased 1D random walk: $f(t) \sim t^{-3/2}$.

If filament dynamics can be well described as a random walk with drift, then the SLT distribution should have the form given by Eq. (2). Figure 3 shows the behavior of $f(t)$ function and compares it to direct simulations of diffusion with drift. Later we demonstrate that a broad class of processes that involves filament polymerization can be described by the diffusion-with-drift model.

2. Microscopic Stochastic Polymerization

One of the simplest models of filament dynamics is a process where monomers stochastically associate and dissociated at one end of the growing filament. Given microscopic association and dissociation rates k_{on} (s^{-1}) and k_{off} (s^{-1}), dynamics of the tip can be considered as a one-step 1D random walk. At times longer than individual events of association and dissociation, dynamics of this process can be described by the Fokker–Plank equation (1) with the drift velocity $V = \delta(k_{on} - k_{off})$ and the effective diffusion coefficient $D = \delta^2(k_{on} + k_{off})/2$, where δ is the length of the monomer.

The FPT distribution is given by Eq. (2) with the characteristic timescale that depends on the association and dissociation rates: $\tau = 4D/V^2 = 2(k_{on} + k_{off})/(k_{on} - k_{off})^2$. For example, at conditions that strongly favor polymerization $\kappa_{on} >> \kappa_{off}$ and $\tau \approx 2/k_{on}$. Note that association rate $k_{on} = \kappa_{on}[M]$ depends on the bimolecular association constant κ_{on} and the concentration of the monomers $[M]$. For example, for isolated tubulin in standard polymerization buffers, $\kappa_{on} \approx 3\,\mu M^{-1}\,s^{-1}$ and at the physiological concentration of tubulin dimers $[M] = 10\,\mu M$ we obtain $k_{on} = \kappa_{on}[M] = 30\,s^{-1}$. In the extract, such concentration of tubulin leads to steady polymerization of microtubules. This estimate of $k_{on} \approx 30\,s^{-1}$ yields the velocity of growth $V = \delta(k_{on} - k_{off}) \approx \delta k_{on} = 8\,nm \times 30\,s^{-1} = 14\,\mu m/min$, which is consistent with the growth velocity of about $10\,\mu m/min$ typically observed in experiments. Using the estimate for $k_{on} \approx 30\,s^{-1}$, we conclude that stochastic association/dissociation dynamics alone would lead to very short speckle lifetime

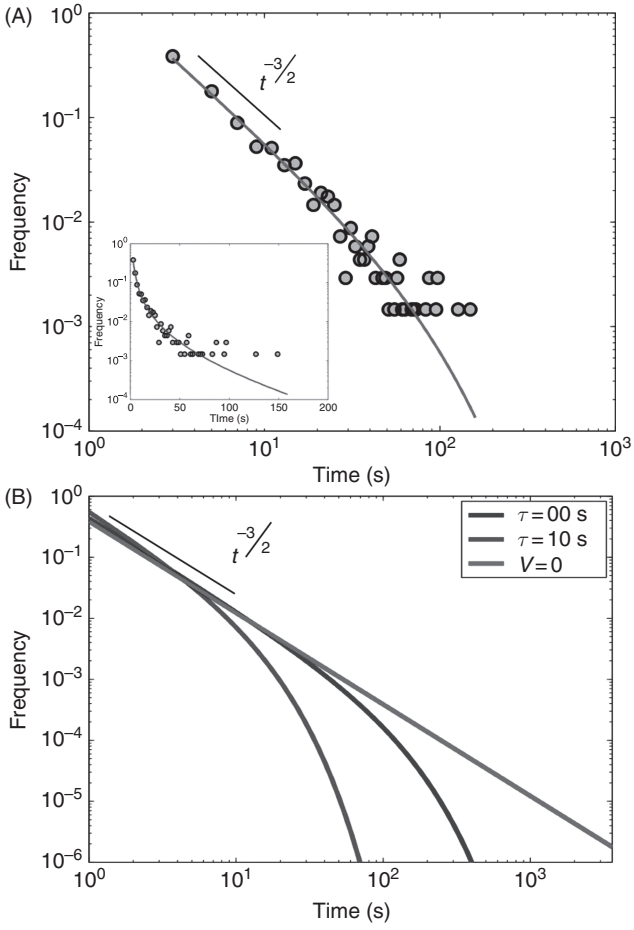

Fig. 3 Speckle-lifetime (SLT) distribution for diffusion with drift. (A) SLT distribution obtained by simulations of diffusion with drift (circles) is well fit by Eq. (2) (red line). The process was simulated as association–dissociation process with continuous time and discrete space. Speckle lifetimes were calculated by randomly picking a monomer at the moment of association and measuring time till its dissociation. (B) SLT distribution computed by Eq. (2) for different values of V and D.

$\tau \approx 2/k_{\text{on}} = 2/(30\,\text{s}^{-1}) = 0.07\,\text{s}$. By comparing this estimate to experimental SLT one can evaluate the role of the microscopic association/dissociation process in filament dynamics.

3. Two-State Model of Microtubule Dynamics

Dynamic instability of microtubules is a process during which periods of steady polymerization (growth) are interrupted by periods of rapid depolymerization (shrinkage) (see Fig. 4). Models of dynamic instability (Dogterom and Leibler, 1993) consider a two-state process that includes stochastic switching between growth and shrinkage states.

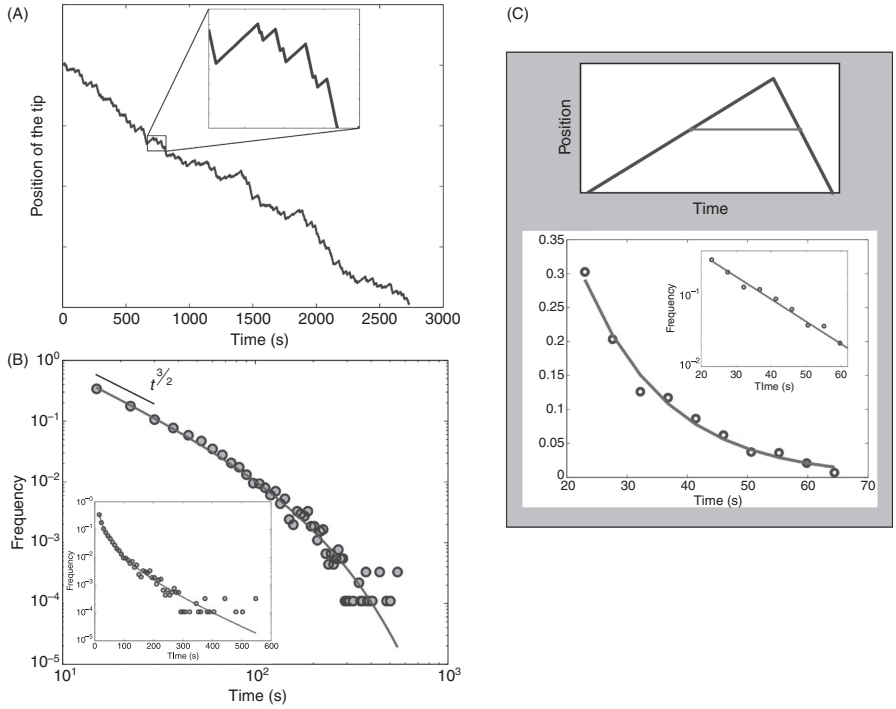

Fig. 4 Dynamic instability. (A) A trajectory of the filament tip obtained by simulating the two-state dynamics. Inset: a fragment of the trajectory. On a longer timescale the process can be considered as diffusion with drift. (B) Simulated SLT distribution obtained for the two-state model of dynamic instability (circles). Equation (2) for diffusion with drift closely fits the data (red line). (C) The two-state model without rescues or other additional sources of fluctuations. The trajectory of a filament (blue) and a single-molecule lifetime (red). Theory predicts that the SLT distribution should be exponential (red line, lower), which is well supported by simulations (blue circles).

According to the two-state model, the microtubule is either growing (plus state) with velocity v_+ or shrinking (minus state) with velocity v_-. The catastrophe, i.e., switching from growing to shrinking, occurs with the rate (probability per unit time) f_-, while the opposite, rescue rate, occurs with the rate f_+ (Dogterom and Leibler, 1993). The FPT distribution for the process has been obtained by Bicout (1997). At timescales longer than individual periods of growth and shrinkage the dynamics of the tip can be described as a 1D random walk with the drift V and effective diffusion coefficient D:

$$V = \frac{f_+ v_+ - f_- v_-}{f_+ + f_-}, \quad D = \frac{v_+ v_-}{f_+ + f_-} \tag{3}$$

The advantage of the random-walk description is that four parameters of the two-state model are aggregated into two coarse parameters: D and V. The value of the diffusion coefficient determines how stochastic the dynamics is, while the velocity of the drift, V, determines whether the filament is growing or shrinking (Bicout, 1997; Redner, 2001).

The speckle lifetime due to dynamic instability should be distributed according to Eq. (2) with a single characteristic of timescale:

$$\tau = \frac{4D}{V^2} = \frac{4v_+v_-(f_+ + f_-)}{(v_+f_+ + v_-f_-)^2} = \frac{4}{\omega}\left[\frac{\overline{v}}{V}\right]^2 \tag{4}$$

where $\omega = f_+ + f_-$ is a characteristic frequency of switching between two regimes and $\overline{v} = \sqrt{v_+v_-}$ is the geometric mean of growth and shrinkage velocities. For example, if velocities $v_+ = 10\,\mu$m/min, $v_- = 20\,\mu$m/min, and rates of switching f_+ $10\,\text{min}^{-1}$, $f_- = 10\,\text{min}^{-1}$, then characteristic timescale of speckle lifetime $\tau \approx 2$ min. Note that dynamic instability leads to a speckle lifetime of the order of minutes, which is different from the millisecond lifetime emerging due to association and dissociation of individual monomers.

Figure 4B demonstrates that the diffusion-with-drift approximation works well for the two-state model. The SLT distribution obtained by simulating the two-state process is well fit by Eq. (2), with τ computed using Eq. (4) and no fitting parameters.

The approximation of two-state process by diffusion with drift is valid if several rounds of growth and shrinkage take place during the time period τ, i.e., when $\tau >> 1/\omega$. From the expression for τ, we see that this condition is satisfied if $\overline{v} \approx v_+ > |V|$, i.e., the drift velocity V is smaller than the velocity of polymerization during the growth phase. This condition is satisfied if catastrophic shrinkage plays a significant role. The inequality above is satisfied even when the filament spends equal amount of time shrinking and growing (in this case the inequality follows from a well-known relationship between the arithmetic mean and the geometric mean).

An advantage of the random-walk description is that several processes that contribute to filament dynamics can be aggregated into the drift-and-diffusion description. For example, such processes as nonexponential distribution of the duration of the growth phase (Odde *et al.*, 1995), nonsynchronous growth of individual protofilaments, and the role of mechanical stress in association–dissociation dynamics can significantly complicate the two-state model, but nevertheless lead to the drift-and-diffusion dynamics at long timescales. Thus characterizing filament dynamics by two macroscopic parameters of the process, D and V, can provide a simple quantitative description of the dynamics, allowing one to compare filament dynamics in different conditions and in different locations or to quantify the effect of drugs and other perturbations.

Note that measurements of the SLD distribution and the value of $\tau = 4D/V^2$do not allow separate inference of the parameters V and D. Nevertheless, τ can serve as an aggregate characteristic of filament dynamics. Drift velocity and diffusion coefficient can be inferred if another characteristic of the filaments is measured. For example, the mean filament length $L = D/|V|$ can be used in conjunction with τ to disentangle D and V.

4. Two-State Model Without Rescue

Another possible mode of dynamics is dynamic instability with steady growth followed by a period of rapid depolymerization, which leads to complete loss of the microtubule. The new microtubule then nucleates and exhibits the same dynamics. This process is equivalent to the two-state model of dynamic instability without

rescue or any additional sources of fluctuation in the polymerization and depolymerization processes. What is the expected SLT for this process and can it be distinguished from other processes?

Figure 4C presents a trajectory of a single microtubule experiencing growth and complete depolymerization and a possible lifetime of a single speckle. From simple geometrical arguments one can see that if the time to catastrophe is t_{-}, then the mean lifetime of a speckle is $t_{-}(1 + v_{+}/v_{-})/2$. Since the waiting time for the catastrophe is exponentially distributed with the mean time $1/f_{-}$, then the lifetime of a speckle is also exponentially distributed with a mean $(1 + v_{+}/v_{-})/2f_{-}$: $f(t) \sim \exp[-2f_{-}t/(1 + v_{+}/v_{-})]$. As shown in Fig. 4C, the SLT distribution obtained in simulations of this process is in very good agreement with the analytical expression.

5. Treadmilling

Polymerization at one end of the filament accompanied by depolymerization at the other end leads to treadmilling dynamics (Margolis *et al*., 1978; Wegner, 1976). In the case of treadmilling, the labeled monomer can associate at the growing end and dissociate at either the growing or the shrinking end of the filament. Here we obtain SLT distribution for treadmilling filaments and demonstrate that it is different from the distribution for dynamic instability at one end.

The main difference is that in the case of treadmilling the speckle can disappear either at the growing or at the shrinking end, whichever reaches it first. In this case the SLT distribution is given by

$$f(t) = f_1(t)S_2(t) + f_2(t)S_1(t) \tag{5}$$

where the index labels the end (1 for growing, 2 for shrinking) and $S_{1,2}(t) = \int_t^\infty f_{1,,2}(u)\mathrm{d}u = 1 - \int_0^t f_{1,,2}(u)\mathrm{d}u$ is the *survival probability* (Redner, 2001), i.e., the probability for a speckle to survive for time t after appearing, if only one end is involved. For example, for the end exhibiting diffusion-with-drift dynamics one obtains the survival probability for a newly associating speckle.

$$S_1(t) = 1 - \int_0^t f_1(t) \approx A\left[\sqrt{\frac{\tau}{t}}\exp\left(-\frac{t}{\tau}\right) - \sqrt{\pi}\,\mathrm{Erfc}\left(\sqrt{\frac{t}{\tau}}\right)\right] \tag{6}$$

where A is a time-independent constant and Erfc is a complementary error function.

If both ends are involved, the probability of surviving for time t is the product of probabilities for the two ends: $S(t) = S_1(t)S_2(t)$, and the SLT distribution is obtained as $f(t) = -\mathrm{d}S(t)/\mathrm{d}t$, which leads to the expression (5). In the case of treadmilling, the contribution of the shrinking end $f_2(t|l)$ and $S_2(t|l)$may depend on the length of a filament l, making the whole SLT distribution depend on the filament length $f(t|l)$. To obtain the distribution for an ensemble of filaments present in the system, one needs to average $f(t|l)$with the distribution of filament length $g(l)$:

$$f(t) = \int_0^\infty f(t|l)g(l)\mathrm{d}l \tag{7}$$

For example, consider a treadmilling process where the growing end is experiencing stochastic dynamics of polymerization and depolymerization and the shrinking end is subject to steady depolymerization at a constant speed $V_0 > 0$. For the shrinking end we obtain $f_2(t|l) = \delta(t - t_0)$ and $S_2(t|l) = 1 - \theta(t - t_0)$, where $t_0 \equiv l/V_0$. Assuming exponential distribution of the filament length $g(l) = \exp(-l/L)/L$ with the mean length L, we get the SLT distribution as follows:

$$f(t) = f_1(t)\left[1 - \exp\left(-\frac{tV_0}{L}\right)\right] + S_1(t)\frac{V_0}{L}\exp\left(-\frac{tV_0}{L}\right) \tag{8}$$

where

$$S_1(t) = \frac{x_0|V|}{2D}\left[\sqrt{\frac{\tau}{t}}\exp\left(-\frac{t}{\tau}\right) - \sqrt{\pi}\,\mathrm{Erfc}\left(\sqrt{\frac{t}{\tau}}\right)\right]$$

and

$$f_1(t) = \frac{x_0}{\sqrt{4\pi D}}t^{-3/2}\exp\left(-\frac{t}{\tau}\right)$$

are the same as for those in Eqs. (2) and (6) with explicit constants and x_0 is the length of the monomer. The treadmilling process also determines the distribution of the filament length. If the shrinking end is depolymerizing faster than the growing end is polymerizing (i.e., $V_0 > V > 0$), then the length of the filament is driven by diffusion with the negative drift $V - V_0$, leading to the exponential distribution of the filament length with the mean length $L = -D/(V - V_0)$.

Figure 5 presents the SLT distribution $f(t)$ for this process. The distribution is clearly different from the SLT distribution for dynamic instability that involves only one end of the filament. In the case of treadmilling, more speckles show long lifetime, which appears when they escape depolymerization at the growing end and wait until the shrinking end reaches them. Short-time behavior is also noticeably different with the power law $\sim t^{-1/2}$for treadmilling, instead of $\sim t^{-3/2}$for dynamic instability. One can also derive an SLT distribution for treadmilling when both ends exhibit diffusion with drift (or dynamic instability).

The SLT distribution obtained can be used to fit single-molecule lifetime data for treadmilling. The shape of the measured lifetime distribution can be used to discriminate between treadmilling and dynamic instability at one end, and in particular, the short-time behavior for these two processes is expected to be different.

C. Connecting to Other Types of Measurements

The distribution of single-molecule lifetimes can be connected to other types of measurements used to characterize filament dynamics, such as FRAP, color replacements, or photoactivation techniques. These experiments measure, as a

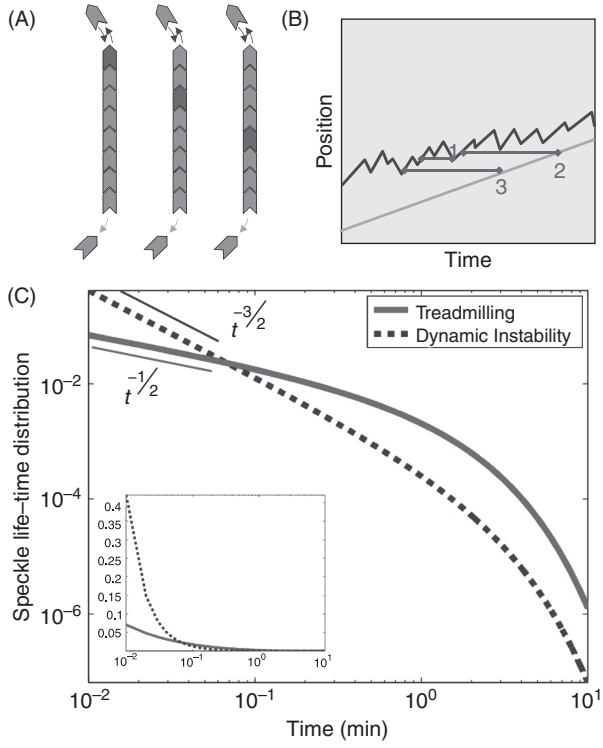

Fig. 5 Treadmilling. (A) Stochastic polymerization at the growing end and depolymerization at the shrinking end can contribute to the speckle lifetime. (B) Trajectories of the growing (blue) and shrinking (orange) ends of the filament, and the three speckles illustrate that the speckle can be lost at the growing end (speckle 1) or the shrinking one (speckles 2 and 3). (C) Comparison of the analytical forms of SLT distributions for treadmilling (red) and dynamic instability (blue). Note that in the case of treadmilling more speckles show longer lifetimes (escape depolymerization of the growing end). At short timescales treadmilling SLT has a slope of –1/2 instead of –3/2 for diffusion with drift. Both distributions have been normalized. The inset shows the same distributions in log–linear axis. Parameters used are as follows: growth velocity 8 μm/min, shrinkage velocity 9 μm/min (treadmilling 1 μm/min), diffusion coefficient 30 μm^2/min (mean length $L = 30$ μm).

function of time, the fraction of monomers that have exchanged with the solvent. SLT distribution, in turn, measures the exchange time for a single monomer that associated at the tip (Fig. 6). Later we demonstrate that color replacement experiments can also provide quantitative information about filament dynamics.

FRAP, photoactivation, and color replacement experiments measure the fraction $G(t)$ of incorporated monomers that have exchanged by time t, after the photobleaching, photoactivation, or saturation with monomers of the second color which took place at $t = 0$. Given FPT distribution $f(t|x)$ one can calculate $G(t)$. Earlier we considered the lifetime of a single molecule from the moment of association until dissociation and demonstrated its equivalence to the time of return of a corresponding random walk. Here we need to consider not only monomers that have just associated, but also those that built the body of the filament. The function $f(t|x)$ is the distribution of the time till the tip of the filament reaches, for the first time, a monomer that has been located distance at a x from the tip at $t = 0$. For 1D diffusion with drift this is given as follows:

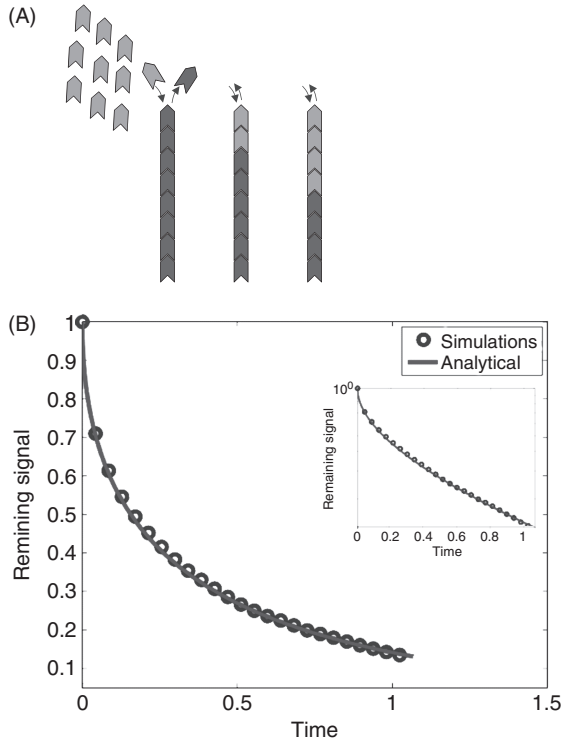

Fig. 6 Monomer exchange in bulk experiments. (A) Dynamics of monomer exchange in a color replacement experiment. (B) Time course of the remaining color. Direct stochastic simulations (blue) have been done for an ensemble of 1000 filaments ($D = 30\,\mu m^2/min$, $V = -8\,\mu m/min$, leading to $\tau = 1.8\,min$ and $L = 3.8\,\mu m$). Analytical expression (Eq. 10) without fit parameters (using τ from simulations) is shown in magenta. Inset: log–linear plot demonstrating that the decay is nonexponential.

$$f(t|x) = \frac{x}{\sqrt{4\pi D}} t^{-3/2} \exp\left(-\frac{(x - Vt)^2}{4Dt}\right) \tag{9}$$

Note that at small x the function $f(t|x)$ takes the familiar form of Eq. (2) discussed earlier. From this expression one can obtain survival probability $S(t|x)$, i.e., the probability that a monomer located at a distance x from the tip at $t = 0$ did not exchange by time t. Since labeled monomers are distributed uniformly in the body of the filament, survival probability has to be integrated over the length of the filament $S(t|l) = \int_0^l S(t|x)\mathrm{d}x$, for a filament of length l. Finally the fraction of remaining monomers is obtained by averaging $S(t|l)$over the distribution $g(l)$ of the filament length. In the case of exponential distribution with mean L that is itself determined by a diffusion-and-drift process (i.e., $L = D/V$), we obtained

$$G(t) = \mathrm{Erfc}\left(\sqrt{\frac{t}{\tau}}\right)\left(1 + 2\frac{t}{\tau}\right) - \frac{2}{\sqrt{\pi}}\sqrt{\frac{t}{\tau}}\exp\left(-\frac{t}{\tau}\right) \tag{10}$$

where τ is the same parameter that could be measured from single-molecule lifetime analysis.

Figure 6 demonstrates that this expression provides an excellent fit to a simulation of the remaining fluorescence in a color replacement experiment. Note that the replacement curve is not a simple exponential, and fitting experimental data to a sum of exponentials—instead of Eq. (10)—would incorrectly suggest the presence of multiple processes with different timescales. If the distribution of the filament length deviates from the exponential generated by diffusion and drift of the filament tip (i.e., $L \neq D/V$), one can use a more general form of Eq. (10) with one more dimensionless parameter, the *Peclet number*, $Pe = LV/D$:

$$G(t) = \frac{1}{2(1+1/Pe)}\left[\mathrm{Erfc}\left(\sqrt{\frac{t}{\tau}}\right) + \exp\left(4\left(\frac{1}{Pe^2}+\frac{1}{Pe}\right)\frac{t}{\tau}\right)\right.$$
$$\left.\times\left(1+\frac{2}{Pe}\right)\mathrm{Erfc}\left(-\left(1+\frac{2}{Pe}\right)\sqrt{\frac{t}{\tau}}\right)\right] \tag{11}$$

Naturally, as $Pe \to -1$ Eq. (11) converges to Eq. (10). The Peclet number inferred from experimental measurements can tell whether the length distribution of the filaments is shaped by the same process that leads to monomer exchanges and can be used to estimate the contributions of other processes (e.g., treadmilling) in filament dynamics.

The connection between SLT distribution and the time course of fluorescence exchange can be used to measure the characteristic timescale of diffusion-and-drift τ. However, care must be taken when interpreting bulk experiments because other processes can also contribute to the measured exchange rate, such as monomer diffusion and rebinding, which are not considered in the models described earlier and are intrinsically excluded from single-molecule lifetime measurements.

IV. Results and Conclusion

The experimentally measured SLT distribution from tubulin molecules in Xenopus extract spindles is shown in Fig. 7, plotted log–log. The data is a power law for short times, going like $\sim t^{-3/2}$. This behavior is consistent with diffusion-with-drift dynamics of microtubule ends by dynamic instability, but is inconsistent with treadmilling being the major mechanism of turnover. Figure 7 also shows that a full fit to Eq. (2) can account for the entire lifetime distribution. When using a least squared fit of the SLT distribution to Eq. (2), it is important to fit the log of the relative frequency to the log of Eq. (2). Directly fitting with a linear axis strongly weighs the short time events, which are far more plentiful than the molecules with long lifetimes, but the information on the correct value of τ resides at long times. The fit to our data gives $\tau = 64 \pm 6$ s. This long timescale cannot be explained solely by

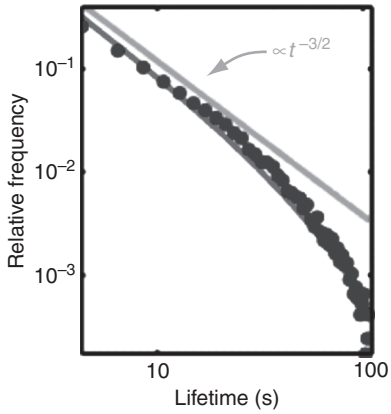

Fig. 7 Single-molecule lifetime distribution. The measured lifetime distribution of single tubulin molecules in Xenopus egg extract spindles (blue). A best fit to Eq. (2) (red line, see text) and a guide to the eye illustrating the $\sim t^{-3/2}$ power law behavior for short lifetimes.

microscopic fluctuations of individual dimers associating and dissociating, which are expected to occur on far faster timescales (see earlier), and thus is most likely dominated by larger length changes of the filament. A τ of 64 s corresponds to a predicted microtubule lifetime of ~16 s, which is very similar to the lifetime of microtubules in Xenopus egg extract far removed from spindles (Belmont *et al*., 1990; Verde *et al*., 1992), arguing that spindle microtubules are not greatly stabilized (Needleman *et al*., 2010).

This technique can also be used to study how microtubule stability in Xenopus extract spindles responds to various molecular perturbations (see Needleman *et al*., 2010 for more details). For example, Fig. 8 shows the SLT distribution in extract

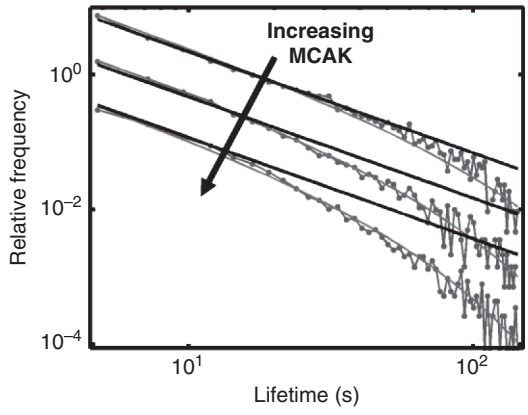

Fig. 8 Single-molecule lifetime distributions change with molecular perturbations. The measured lifetime distribution of single tubulin molecules in Xenopus egg extract spindles with 50% MCAK, 100% MCAK, and 200% MCAK (blue). Best fits to Eq. (2) (red line, see text) and guides to the eye illustrating the $\sim t^{-3/2}$ power law behavior for short lifetimes (black lines). The curves have been shifted along the vertical axis to facilitate comparison and simultaneous viewing.

spindles assembled with various concentrations of mitotic centromere-associated kinesin (MCAK), a microtubule depolymerizer. MCAK was depleted from the extract and recombinant MCAK was added back to 50, 100, and 200% native levels. Fitting the corresponding SLT distributions to Eq. (2) gave $\tau = 97 \pm 11$ s, $\tau = 61 \pm 5$ s, and $\tau = 47 \pm 3$ s, quantifying how the concentration of MCAK effects the turnover of microtubules in extract spindles.

Single-molecule measurements provide a powerful tool to study protein dynamics *in vitro* and *in vivo*. However, it can be difficult to relate results of these measurements to the underlying physical processes of interest. In this chapter, we presented a theoretical framework to interpret single-molecule measurements on cytoskeletal filaments. We showed that the lifetime distribution of monomers in the filament corresponds to the FPTs of the filaments ends. This allowed us to compute the expected shape of the single-molecule lifetime distribution for different models of filament dynamics. Even for very simple models, these lifetime distributions have nontrivial shapes: they are not exponential or sums of exponentials. We demonstrate that the measured lifetime distribution of tubulin molecules in Xenopus egg extract spindles can be quantitatively described by a model in which spindle microtubules grow and shrink with diffusion-with-drift dynamics. This allowed us to quantify the stability of microtubules in spindles and measure the effects of molecular perturbations. This same framework should provide a powerful tool for interpreting single-molecule measurements from cytoskeletal filaments in other contexts (Watanabe and Mitchison, 2002).

References

Alberts, B., Johnson, A., Lewis, J., Raff, M., Roberts, K., and Walter, P. (2008). "Molecular Biology of the Cell." Garland Science, New York, NY.

Belmont, L. D., Hyman, A. A., Sawin, K. E., and Mitchison, T. J. (1990). Real-time visualization of cell cycle-dependent changes in microtubule dynamics in cytoplasmic extracts. *Cell* **62**, 579–589.

Bicout, D. J. (1997). Green's function and first passage time distribution for dynamic instability of microtubules. *Phys. Rev. E* **56**, 6656.

Crocker, J. C., and Grier, D. G. (1996). Methods of digital video microscopy for colloidal studies. *J. Colloid. Interface Sci.* **179**, 298–310.

Dogterom, M., and Leibler, S. (1993). Physical aspects of the growth and regulation of microtubule structures. *Phys. Rev. Lett.* **70**, 1347.

Dumont, S., and Mitchison, T. J. (2009). Force and length in the mitotic spindle. *Curr. Biol.* **19**, R749–R761.

Hannak, E., and Heald, R. (2006). Investigating mitotic spindle assembly and function *in vitro* using *Xenopus laevis* egg extracts. *Nat. Protoc.* **1**, 2305–2314.

Hyman, A. A., Drechsel, D., Kellogg, D., Salser, S., Sawin, K. E., Steffen, P., Wordeman, L., and Mitchison, T. J. (1991). Preparation of modified tubulins. *Meth. Enzymol.* **196**, 478–485.

Inoue, S., and Sato, H. (1967). Cell motility by labile association of molecules. The nature of mitotic spindle fibers and their role in chromosome movement. *J. Gen. Physiol.* **50**, 259–292.

Jaqaman, K., Loerke, D., Mettlen, M., Kuwata, H., Grinstein, S., Schmid, S. L., and Danuser, G. (2008). Robust single-particle tracking in live-cell time-lapse sequences. *Nat. Methods* **5**, 695–702.

Kueh, H. Y., and Mitchison, T. J. (2009). Structural plasticity in actin and tubulin polymer dynamics. *Science* **325**, 960–963.

Margolis, R. L., Wilson, L., and Keifer, B. I. (1978). Mitotic mechanism based on intrinsic microtubule behavior. *Nature* **272**, 450–452.

Needleman, D. J., Groen, A. C., Ohi, R., Maresca, T. J., Mirny, L., and Mitchison, T. J. (2010). Fast microtubule dynamics in meiotic spindles measured by single molecule imaging: Evidence that the spindle environment does not stabilize microtubules. *Mol. Biol. Cell* **21**, 323–333.

Niethammer, P., Kueh, H. Y., and Mitchison, T. J. (2008). Spatial patterning of metabolism by mitochondria, oxygen, and energy sinks in a model cytoplasm. *Curr. Biol.* **18**, 586–591.

Odde, D. J., Cassimeris, L., and Buerrner, H. M. (1995). Kinetics of microtubule catastrophe assessed by probabilistic analysis. *Biophys. J.* **69**, 796–802.

Redner, S. (2001). "A Guide to First-Passage Processes." Cambridge University Press, Cambridge, UK.

Salmon, E. D., Leslie, R. J., Saxton, W. M., Karow, M. L., and McIntosh, J. R. (1984). Spindle microtubule dynamics in sea urchin embryos: Analysis using a fluorescein-labeled tubulin and measurements of fluorescence redistribution after laser photobleaching. *J. Cell Biol.* **99**, 2165–2174.

Sawin, K. E., and Mitchison, T. J. (1991). Poleward microtubule flux in mitotic spindles assembled *in vitro*. *J. Cell Biol.* **112**, 941–954.

Serge, A., Bertaux, N., Rigneault, H., and Marguet, D. (2008). Dynamic multiple-target tracing to probe spatiotemporal cartography of cell membranes. *Nat. Methods* **5**, 687–694.

Valloton, P., Ponti, A., Waterman-Storer, C. M., Salmon, E. D., and Danuser, G. (2003). Recovery, visualization, and analysis of actin and tubulin polymer flow in live cells: A fluorescent speckle microscopy study. *Biophys. J.* **85**, 1289–1306.

Verde, F., Dogterom, M., Stelzer, E., Karsenti, E., and Leibler, S. (1992). Control of microtubule dynamics and length by cyclin a- and cyclin b-dependent kinases in xenopus egg extracts. *J. Cell Biol.* **118**, 1097–1108.

Watanabe, N., and Mitchison, T. J. (2002). Single-molecule speckle analysis of actin filament turnover in lamellipodia. *Science* **295**, 1083–1086.

Wegner, A. (1976). Head to tail polymerization of actin. *J. Mol. Biol.* **108**, 139–150.

Yang, G., Houghtaling, B. R., Gaetz, J., Liu, J. Z., Danuser, G., and Kapoor, T. M. (2007). Architectural dynamics of the meiotic spindle revealed by single-fluorophore imaging. *Nat. Cell Biol.* **9**, 1233–1242.